# A nanoscale gigahertz source realized with Josephson scanning tunneling microscopy

Berthold Jäck' , Matthias Eltschka, Maximilian Assig, Andreas Hardock, Markus Etzkorn, Christian R. Ast, and Klaus Kern

Citation: Appl. Phys. Lett. **106**, 013109 (2015); doi: 10.1063/1.4905322
View online: http://dx.doi.org/10.1063/1.4905322
View Table of Contents: http://aip.scitation.org/toc/apl/106/1
Published by the American Institute of Physics



# A nanoscale gigahertz source realized with Josephson scanning tunneling microscopy

Berthold Jäck,[1,a)] Matthias Eltschka,[1] Maximilian Assig,[1] Andreas Hardock,[2] Markus Etzkorn,[1] Christian R. Ast,[1] and Klaus Kern[1,3]
[1]*Max-Planck-Institut für Festkörperforschung, 70569 Stuttgart, Germany*
[2]*Institut für Theoretische Elektrotechnik, Technische Universität Hamburg-Harburg, 21079 Hamburg, Germany*
[3]*Institut de Physique de la Matière Condensée, Ecole Polytechnique Fédérale de Lausanne, 1015 Lausanne, Switzerland*

(Received 30 October 2014; accepted 18 December 2014; published online 6 January 2015)

Using the AC Josephson effect in the superconductor-vacuum-superconductor tunnel junction of a scanning tunneling microscope (STM), we demonstrate the generation of GHz radiation. With the macroscopic STM tip acting as a $\lambda/4$-monopole antenna, we first show that the atomic scale Josephson junction in the STM is sensitive to its frequency-dependent environmental impedance in the GHz regime. Further, enhancing Cooper pair tunneling via excitations of the tip eigenmodes, we are able to generate high-frequency radiation. We find that for vanadium junctions, the enhanced photon emission can be tuned from about 25 GHz to 200 GHz and that large photon flux in excess of $10^{20}\,\mathrm{cm}^{-2}\,\mathrm{s}^{-1}$ is reached in the tunnel junction. These findings demonstrate that the atomic scale Josephson junction in an STM can be employed as a full spectroscopic tool for GHz frequencies on the atomic scale. © *2015 AIP Publishing LLC*.
[http://dx.doi.org/10.1063/1.4905322]

The frequency band ranging from GHz to THz frequencies is extensively used to probe charge carriers and their spin dynamics in solids and rotational motions of molecules, addressing problems in biology, physics, and astronomy.[1–3] It is of particular interest to introduce this frequency range into the vivid research field of nanoscale science, in order to investigate nanoscale objects, such as individual molecular magnets,[4] and the physics of individual nuclear as well as electronic spins.[5,6] However, generating and guiding this radiation requires adaptation to the experimental conditions of local probe experiments, like scanning tunneling microscope (STM), for instance, adding another level of complexity. To date, all realizations of an STM employing high frequency (HF) radiation feed externally generated HF-signals into the junction by means of optical guiding or waveguides.[7,8]

In this study, we circumvent the external feed by exploiting the AC Josephson effect in the tunnel junction of an STM.[9,10] High-frequency radiation can both be generated and detected by the AC Josephson effect, which acts as a perfect voltage $U$ to frequency $\nu$ converter through the relation $h\nu = 2eU$—in a simplified picture describing inelastic Cooper pair tunneling. Moreover, Josephson junctions with small junction capacity $C_J$, as is the case for an STM tunnel junction, reveal a high sensitivity to their electromagnetic environment.[11] These unique properties of the AC Josephson effect in combination with the local probe capabilities of an STM make the AC Josephson STM an ideal broadband atomic scale spectroscopy tool under UHV conditions.

Here, we show how a Josephson junction in an STM couples directly to the immediate electromagnetic environment. We use a thin vanadium (V) wire (250 $\mu$m diameter) as STM tip and a V(100) sample to create a nanoscale Josephson junction as shown in Fig. 1(a). Experiments are carried out in an STM operating at a base temperature of $T = 15$ mK,[12] so that both tip and sample are well in the superconducting state.[13] Moreover, we show that the STM tip acts as a monopole antenna through the coupling between the Josephson junction and its environment. The tip's frequency-dependent impedance enhances Cooper pair tunneling at resonance facilitating the generation of a large photon field in the tunnel contact.

Fig. 1(b) displays the measured in-gap tunneling current-voltage spectrum $I(U)$ of a voltage-biased Josephson junction using an $l = 1.7 \pm 0.1$ mm long STM tip. It exhibits a prominent supercurrent peak at about $\pm 14$ $\mu$V, which is a signature of the DC Josephson effect usually occurring at zero bias voltage. Here, fluctuations of the phase coherence between the two superconducting electrodes imposed by thermal noise in the environment shift this peak to finite bias, as reported for STM experiments before.[14–17] In addition, the $I(U)$-spectrum features several current peaks at higher bias voltages labeled $\nu_{1,2,3}$. Their position does not depend on temperature, on magnetic field, nor on the normal state tunneling resistance. We further investigated the in-gap differential conductance spectrum $dI/dU$ of the tunnel junction, which is shown in Fig. 1(c). For different superconducting order parameters $\Delta_{tip}$ of the tip, we find different voltage positions $eU = \Delta_{tip}$ of the Andreev reflections. The positions of the current peaks $\nu_{1,2,3}$, however, remain unchanged. Therefore, we can exclude these features to originate from multiple Andreev reflections.[18] In the following, we will show that the current peaks represent the eigenmode spectrum of the STM tip acting as a monopole antenna.

Schematically, the tunnel process is shown in Fig. 2(a), where a tunneling Cooper pair disposes of excess kinetic

a)Author to whom correspondence should be addressed. Electronic mail: b.jaeck@fkf.mpg.de

 

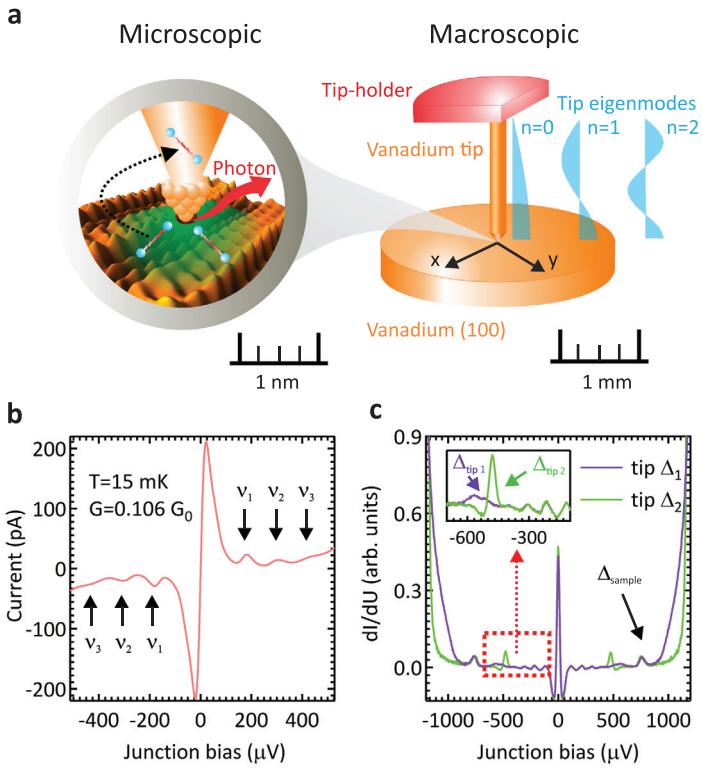


FIG. 1. (a) Comparison of microscopic and macroscopic structures and processes: The macroscopic picture shows the vanadium tip attached to the copper tip-holder which together forms the monopole antenna. The Josephson junction is created with the V(100) sample beneath the STM tip. The electromagnetic eigenmodes of this structure, $n = 0$, 1, and 2 are depicted in blue. The close-up illustrates the microscopic process of Cooper pair tunneling and accompanying photon generation in the atomic scale tunnel contact of STM tip and sample. The sample topography shows the $5 \times 1$ surface reconstruction of the vanadium (100) sample measured at $U = 2.5$ mV and $I = 5$ nA. (b) Current-voltage spectrum of a voltage-biased Josephson junction in an STM measured at a conductance of $G = 0.106 G_0$, with $G_0$ as the quantum of conductance, and at a temperature of $T = 15$ mK. The black arrows indicate the tip eigenmodes $\nu_n$ that correspond to the resonant current features. (c) In-gap differential conductance spectra for measurements with two different tip order parameter $\Delta_{tip}$, but for the same macroscopic tip and at same experimental conditions ($T = 15$ mK and $G = 0.03 G_0$). The order parameter is depending on the mesoscopic tip shape that we modified applying bias voltage pulses. The Andreev reflections corresponding to the sample order parameter $\Delta_{sample}$ and tip order parameter $\Delta_{tip}$ are indicated. The inset is a close-up of the $dI/dU$-signal in the red box.

energy $2eU$ by emitting a photon of energy $h\nu = 2eU$. Resonances in the electromagnetic environment facilitate Cooper pair tunneling, which can be detected as current peaks in the spectrum. The best framework to quantitatively describe a nanoscale Josephson junction of small capacitance, as is the case in the STM, is the $P(E)$-theory.[11,19,20] Here, the Cooper pair tunneling current is described as $I(U) = (\pi\hbar I_0^2/4e) \times [P(2eU) - P(-2eU)]$, where $\hbar$ is the reduced Planck's constant, $e$ is the elementary charge, $I_0$ denotes the critical Josephson current, and $P(E)$ is the probability for a Cooper pair to emit ($E > 0$) or absorb ($E < 0$) a photon of energy $E = h\nu = 2eU$. The only input needed is an analytic description of the environmental excitation spectrum, which in P($E$)-theory is treated as a complex, frequency-dependent impedance $Z(\nu)$.

In the STM, the immediate environment of the Josephson junction is the tip, tip-holder, and the sample. As the contact of tip and tip-holder is low-ohmic and the tunnel contact to the sample is high-ohmic ($R_T = 10^4$–$10^6\ \Omega$), we approximate the tip assembly as open-ended. Thus, the STM tip has the electric properties of a $\lambda/4$-monopole antenna, commonly used for broadcasting applications. In this sense, the tip-holder forms the "antenna ground plane" (see Fig. 1(a)).[21] The STM tip shares a similar eigenfrequency spectrum with resonances at about $\nu_n = (2n + 1) \times c/(4(l + l_0))$, $n = 0$, 1, 2. Here, $c$ denotes the speed of light and $l$ is the tip length with an extension $l_0$ corresponding to an electrical lengthening of the tip.[22,23] The schematic electric field pattern derived from this impedance analysis is also shown for the three lowest eigenmodes $\nu_{0,1,2}$ in Fig. 1(a). For the calculations within the $P(E)$-theory, we can approximate the impedance of the monopole antenna by an open-ended transmission line impedance having an effective resistance and the corresponding eigenfrequency spectrum.[24]

The fit of the total Cooper pair current spectrum with the $P(E)$-theory is shown in Fig. 2(b).[24–26] We find good agreement in the low-frequency region of the supercurrent peak as well as in the high-frequency region of the spectral resonances. The resonant current features relate directly to the employed impedance spectrum $Z(\nu)$, confirming the coupling between Josephson junction and tip eigenmodes. The absolute amplitude of the entire $I(U)$ spectrum is determined by the critical Josephson current $I_0$. The values obtained from the fits at different tunnel conductances are shown in Fig. 2(c). They are in good agreement with the calculated values from theory,[24,27] which validates the consistency of the fit parameters. By contrast, the actually measured supercurrent peak height $I_{SCP}$, shown in Fig. 2(c), is much smaller than the fitted critical current $I_0$ typical for underdamped junction dynamics.[28,29] This observation is consistent with the small

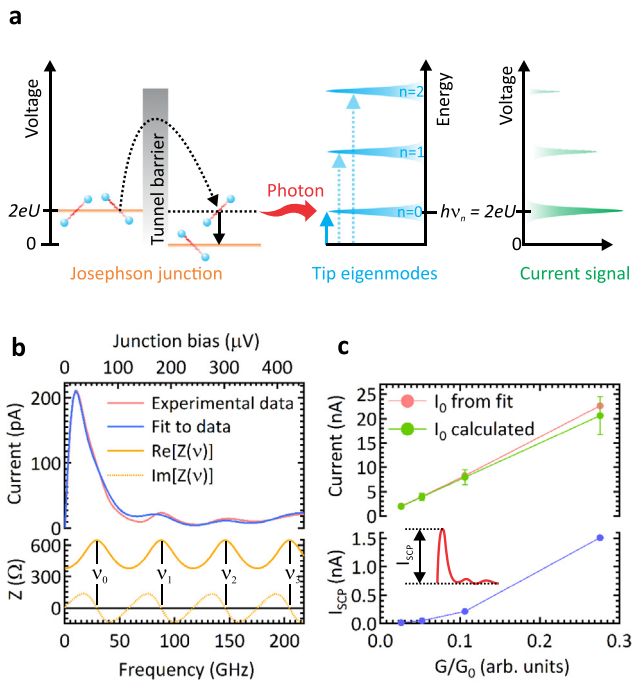


FIG. 2. (a) The left part depicts the conversion of a bias voltage $2eU$ into a photon of energy $h\nu_n$ upon Cooper pair tunneling. The center part shows the excitation of the tip eigenmodes $n = 0$, 1, and 2 and on the right, the expected measurement signal $I(U)$ is shown schematically. (b) $P(E)$-theory based fit to experimental data taken at $T = 15$ mK and $G = 0.11G_0$. The complex impedance $Z(\nu)$ used for the fit is shown below, whose resonance modes—the tip eigenmodes—are labeled $\nu_{0,1,2,3}$. (c) The top graph shows the fitted and calculated critical current values $I_0$ for measurements at different tunnel conductances taken at $T = 15$ mK. The corresponding experimental supercurrent peak amplitude $I_{SCP}$—determined as indicated—is shown below.

total shunt capacity found from the fit $C = 6.31 \pm 0.11$ fF, comprising the junction capacity $C_J$ (typically on the order of femtofarad) and a small albeit unknown contribution from the residual wire capacity. The extremely small capacitive shunt promotes fluctuation-induced, premature switching from the zero voltage DC Josephson state. The underdamped dynamics is of elementary importance for our concept: It redistributes the spectral weight of the tunneling probability $P(E)$ away from the zero voltage state into the finite voltage regime. This redistribution yields sensitivity of the junction to high frequency signals, which is necessary in order to implement the AC Josephson effect as a spectrometer on the atomic scale.[24]

We can use this new insight to tune the position of the resonance current peaks in the nanoscale Josephson junction by changing the length of the tip on a macroscopic scale. In this way, we can deliberately enhance or decrease the Cooper pair tunneling current in specific parts of the spectrum. To demonstrate this control, we have measured $I(U)$ spectra for different tip lengths from $l = 2.7 \pm 0.1$ mm to $l = 0.7 \pm 0.1$ mm shown in Fig. 3(a). It can be clearly seen that the resonances move to higher energies as the tip length is reduced. The highest measured current peaks correspond to resonance frequencies exceeding 200 GHz. Moreover, the electric properties of a monopole antenna are sensitive to the geometry of the tip holder, i.e., the antenna ground plane, as it forms an electric counterweight to the antenna.[22] To demonstrate its impact, we changed the tip-holder surface area, which is shown in Fig. 3(b). While the antenna length, $l = 0.7 \pm 0.1$ mm, stayed the same, the surface area was increased by a factor of 3. For the larger surface area, the peak amplitude more than doubles, almost reaching the supercurrent peak, whereas the tip eigenfrequency $\nu_0$ does not change. We can explain this by the improved properties of the antenna resulting in more efficient coupling to the Josephson junction.

The lowest resonance frequencies $\nu_0$ for the different measured tips and tip-holder shapes are shown in Fig. 3(c) as a function of tip length. They nicely follow the inverse proportionality expected and from the fit, we can extract a value for the electrical lengthening of $l_0 = 0.46 \pm 0.04$ mm. We find similar values for $\nu_0$ from simulations using the finite integral method on the electromagnetic properties of the tip-sample assembly—including tip, tip-holder, and sample.[24] The values found from the simulations are also plotted in Fig. 3(c). We find largely good agreement between experiment and simulations also concerning the effect of electrical lengthening.[22,23] In addition, the electric field pattern of the first three antenna eigenmodes is shown in Fig. 3(d). They resemble the simplified electric field pattern in Fig. 1(a), which we derived from a basic, geometric impedance distribution analysis. In the far field, the tip is expected to radiate with the broad emission angle of a monopole antenna. The

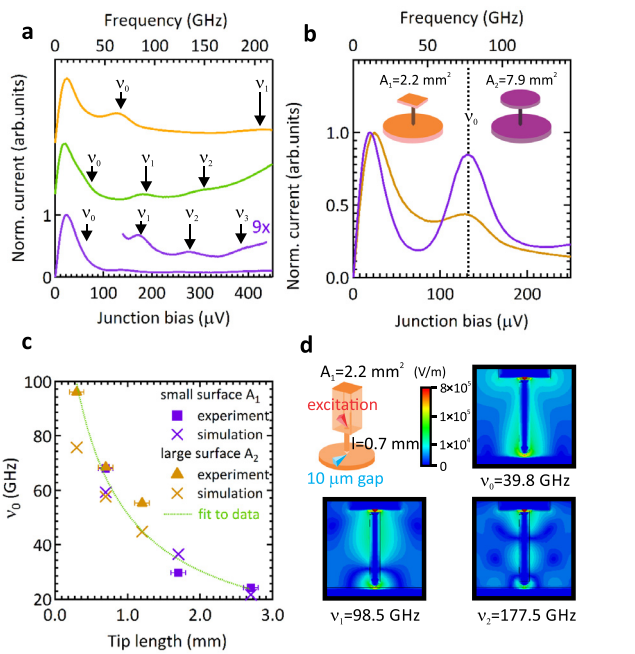


FIG. 3. (a) Experimental $I(U)$ spectra, normalized to the supercurrent peak, for three different tip lengths $l_1 = 2.7 \pm 0.1$ mm, $l_2 = 1.7 \pm 0.1$ mm, and $l_3 = 0.7 \pm 0.1$ mm from bottom to top, respectively. The arrows indicate the resonant current features and the corresponding tip eigenmodes $\nu_n$. (b) Experimental $I(U)$ spectra, normalized to the supercurrent peak, for measurements with two tip-holders of different surface area, which are sketched in the inset (corresponding colour). For both measurements, the tip had the length $l = 0.7 \pm 0.1$ mm. (c) Fitted and simulated tip eigenmode frequency $\nu_0$ vs. tip length l for all tip-assembly geometries used and the fit to the experimental data. (d) Simulated electric field pattern for the three lowest eigenmodes $\nu_{0,1,2}$ of a $l = 1.7$ mm long tip. The structure used for the simulation also shows the port of excitation and indicates the small space between tip apex and sample surface, mimicking the tunnel gap.

field strength is highest at the tip apex. Due to the confined geometry, we estimate that the near field at the tip apex, i.e., in the tunnel junction, to be much larger than the field strength found from simulations. By reciprocity, the antenna is most susceptible to absorb radiation at this point, thereby corroborating the observed strong coupling to the Josephson junction. It can also be seen that the antenna ground plane shows enhanced field strength for every mode, which illustrates its relevance and the impact observed in our experiments (Fig. 3(b)).

In view of the resonator properties of the STM tip and the maximum electric field at the tip apex, we look again at the inelastic tunneling process of Cooper pairs in more detail: The frequency $h\nu$ of the emitted photons can be directly tuned by the applied bias voltage $U$ ($2eU = h\nu$). The tip eigenmode spectrum enhances the tunneling probability of Cooper pairs at specific eigenmode energies $h\nu_n$. This means that the tip eigenmode spectrum facilitates the creation of a photon field in the tunnel junction. Remarkably, while tunnel process as well as photon generation are localized in the nano-scale tunnel contact of the STM, the macroscopic resonator, i.e., the STM tip assembly, necessary to enhance the tunnel process, can be manipulated on the millimeter scale (see Fig. 1(a)). In conjunction with the unity quantum yield of photon generation, these two different length scales facilitate a high photon flux $\phi$ localized at the tunnel contact. For standard experimental conditions, $G = 0.18G_0$, we find lower and upper boundaries of $10^{20} \leq \phi \leq 10^{24}\,\mathrm{cm}^{-2}\,\mathrm{s}^{-1}$, depending on whether we assume emission to occur in the tunnel contact or within the superconducting coherence length.[13,24] These flux values are well within the range of flux applied in conventional laser spectroscopy methods so that we underline the potential of our approach to be employed as a high-frequency source. Our findings represent a realization of AC Josephson spectroscopy in an STM, a method that has already been successfully employed on planar tunnel junction devices.[31,32] The spectrometer frequency is always given by the applied bias voltage that can be tuned externally. The spectral regions of enhanced photon generation are determined by the STM tip length. Hence, in order to cover the entire spectral range of interest, the next step would be to devise an efficient broad band resonator that enhances the emission specifically for spectroscopic applications.

The key properties of the AC Josephson STM spectrometer are its frequency range and its linewidth. The accessible frequency range is limited by the superconducting order parameter $\Delta$ of the electrode material. It could be extended into the THz range by choosing materials with larger $\Delta$ such as $MgB_2$.[30] However, in that case, the junction capacitance and wire resistance have to be adapted to the higher frequency range. The linewidth of the spectrometer is limited by the voltage noise $u$ due to thermal charge fluctuations in the shunting capacitance $\sqrt{\overline{u^2}} = \sqrt{k_B T/C}$. Hence, lowest temperatures are necessary in order to minimize the linewidth. For our current setup, we estimate voltage fluctuations of about $\sqrt{\overline{u^2}} \leq 12\,\mu\mathrm{eV}$.[12] Inserting a larger capacitive shunt will strongly decrease the linewidth but in turn also decrease the junction sensitivity to large frequencies, so that the right shunt needs to be chosen in view of the perspective application. Nevertheless, we have shown that Josephson spectrometry is, in principle, possible on the nanoscale. Together with the local probe capabilities of the STM, we are one step closer to investigate a myriad of nanosystems whose excitation spectrum is the GHz range. Examples of such systems in the spotlight of the scientific community are single magnetic molecules[4,33] or the detection of an individual nuclear spin.[5,34]

In summary, we have shown that a macroscopic STM tip can be employed as a monopole antenna to control the quantum mechanical tunnel process of Cooper pairs in the nano-world. Demonstrating the tip's electromagnetic eigenmodes to induce Cooper pair tunneling through the atomic scale Josephson junction, we deliver direct proof for the AC Josephson effect with an STM. Combining the exceptional properties of the AC Josephson effect with the virtues of an STM, we realize a scannable nanoscale light source of GHz radiation. It operates at high photon flux and over a wide spectral range. In conjunction with the sensing properties of the AC Josephson effect, we demonstrate an alternative approach towards spectroscopy of GHz to THz-signals on the nanoscale.

We gratefully acknowledge helpful discussions with C. Urbina, G.-L. Ingold, and H. Baberschke. C. R. Ast acknowledges funding from the Emmy-Noether-Program of the Deutsche Forschungsgemeinschaft (DFG).

[1]D. Grischkowsky, S. Keiding, M. v. Exter, and C. Fattinger, J. Opt. Soc. Am. B **7**, 2006 (1990).
[2]F. Lucia, *Springer Series in Optical Sciences* (Springer, Berlin, Heidelberg, 2003), Vol. 85, p. 39.
[3]M. C. Beard, G. M. Turner, and C. A. Schmuttenmaer, J. Phys. Chem. B **106**, 7146 (2002).
[4]L. Bogani and W. Wernsdorfer, Nat. Mater. **7**, 179 (2008).
[5]J. M. Elzerman, R. Hanson, L. H. Willems van Beveren, B. Witkamp, L. M. K. Vandersypen, and L. P. Kouwenhoven, Nature **430**, 431 (2004).
[6]P. Neumann, J. Beck, M. Steiner, F. Rempp, H. Fedder, P. R. Hemmer, J. Wrachtrup, and F. Jelezko, Science **329**, 542 (2010).
[7]T. L. Cocker, V. Jelic, M. Gupta, S. J. Molesky, J. A. L. Burgess, G. De Los Reyes, L. V. Titova, Y. Y. Tsui, M. R. Freeman, and F. A. Hegmann, Nat. Photonics **7**, 620 (2013).
[8]U. Kemiktarak, T. Ndukum, K. C. Schwab, and K. L. Ekinci, Nature **450**, 85 (2007).
[9]B. D. Josephson, Phys. Lett. **1**, 251 (1962).
[10]S. Shapiro, Phys. Rev. Lett. **11**, 80 (1963).
[11]D. Averin, Y. Nazarov, and A. A. Odintsov, Physica B **165–166**, 945 (1990).
[12]M. Assig, M. Etzkorn, A. Enders, W. Stiepany, C. R. Ast, and K. Kern, Rev. Sci. Instrum. **84**, 033903 (2013).
[13]S. T. Sekula and R. H. Kernohan, Phys. Rev. B **5**, 904 (1972).
[14]Y. M. Ivanchenko and L. A. Zil'berman, ZhETF **55**, 2395 (1969) [Sov. Phys. JETP **28**, 1272 (1969)].
[15]O. Naaman, W. Teizer, and R. Dynes, Phys. Rev. Lett. **87**, 097004 (2001).
[16]J. G. Rodrigo, V. Cresp, and S. Vieira, Physica C **437**, 270 (2006).
[17]N. Bergeal, Y. Noat, T. Cren, T. Proslier, V. Dubost, F. Debontridder, A. Zimmers, D. Roditchev, W. Sacks, and J. Marcus, Phys. Rev. B **78**, 140507 (2008).
[18]T. Klapwijk, G. Blonder, and M. Tinkham, Physica B+C **109–110**, 1657 (1982).
[19]M. Devoret, D. Esteve, H. Grabert, G.-L. Ingold, H. Pothier, and C. Urbina, Phys. Rev. Lett. **64**, 1824 (1990).
[20]T. Holst, D. Esteve, C. Urbina, and M. H. Devoret, Physica B **203**, 397 (1994).
[21]To clarify the terminology, the tip-holder acts effectively as the antenna ground plane although in the STM the tip holder is actually not connected to ground.
[22]J. S. Belrose, *The Handbook of Antenna Design* (Peter Peregrinus Ltd., London, 1983), Chap. 15.
[23]G. H. Brown and O. M. Woodward, Jr., Proc. IRE **33**, 257 (1945).

[24]See supplementary material at http://dx.doi.org/10.1063/1.4905322 for more details on the implementation of $P(E)$-theory, calculation of $I_0$, Josphson junction phase dynamics, finite integral method simulation, and calculation of the photon density.
[25]G.-L. Ingold and H. Grabert, Europhys. Lett. **14**, 371 (1991).
[26]G.-L. Ingold, H. Grabert, and U. Eberhardt, Phys. Rev. B **50**, 395 (1994).
[27]V. Ambegaokar and A. Baratoff, Phys. Rev. Lett. **10**, 486 (1963).
[28]D. E. McCumber, J. Appl. Phys. **39**, 3113 (1968).
[29]W. C. Stewart, Appl. Phys. Lett. **12**, 277 (1968).
[30]J. Nagamatsu, N. Nakagawa, T. Muranaka, Y. Zenitani, and J. Akimitsu, Nature **410**, 63 (2001).
[31]K. Baberschke, K. Bures, and S. Barnes, Phys. Rev. Lett. **53**, 98 (1984).
[32]L. Bretheau, Ç. Girit, H. Pothier, D. Esteve, and C. Urbina, Nature **499**, 312 (2013).
[33]B. W. Heinrich, L. Braun, J. I. Pascual, and K. J. Franke, Nat. Phys. **9**, 765 (2013).
[34]R. Vincent, S. Klyatskaya, M. Ruben, W. Wernsdorfer, and F. Balestro, Nature **488**, 357 (2012).